

Manno-oligosaccharides from cassia seed gum ameliorate inflammation and improve glucose metabolism in diabetic rats

Chenxuan Wu ^{a, #}, Jun Liu ^{a, #}, Yanxiao Li ^b, Nannan Wang ^a, Qiaojuan Yan ^b, Zhengqiang Jiang ^{a, *}

^a Key Laboratory of Food Bioengineering (China National Light Industry), College of Food Science and Nutritional Engineering, China Agricultural University, Beijing 100083, China

^b Department of Nutrition and Health, College of Engineering, China Agricultural University, Beijing 100083, China

Authors contribute equally to this work.

* Corresponding author: Z.Q. Jiang

Tel.: +86 10 62737689; Fax: +86 10 82388508

E-mail: zhqjiang@cau.edu.cn

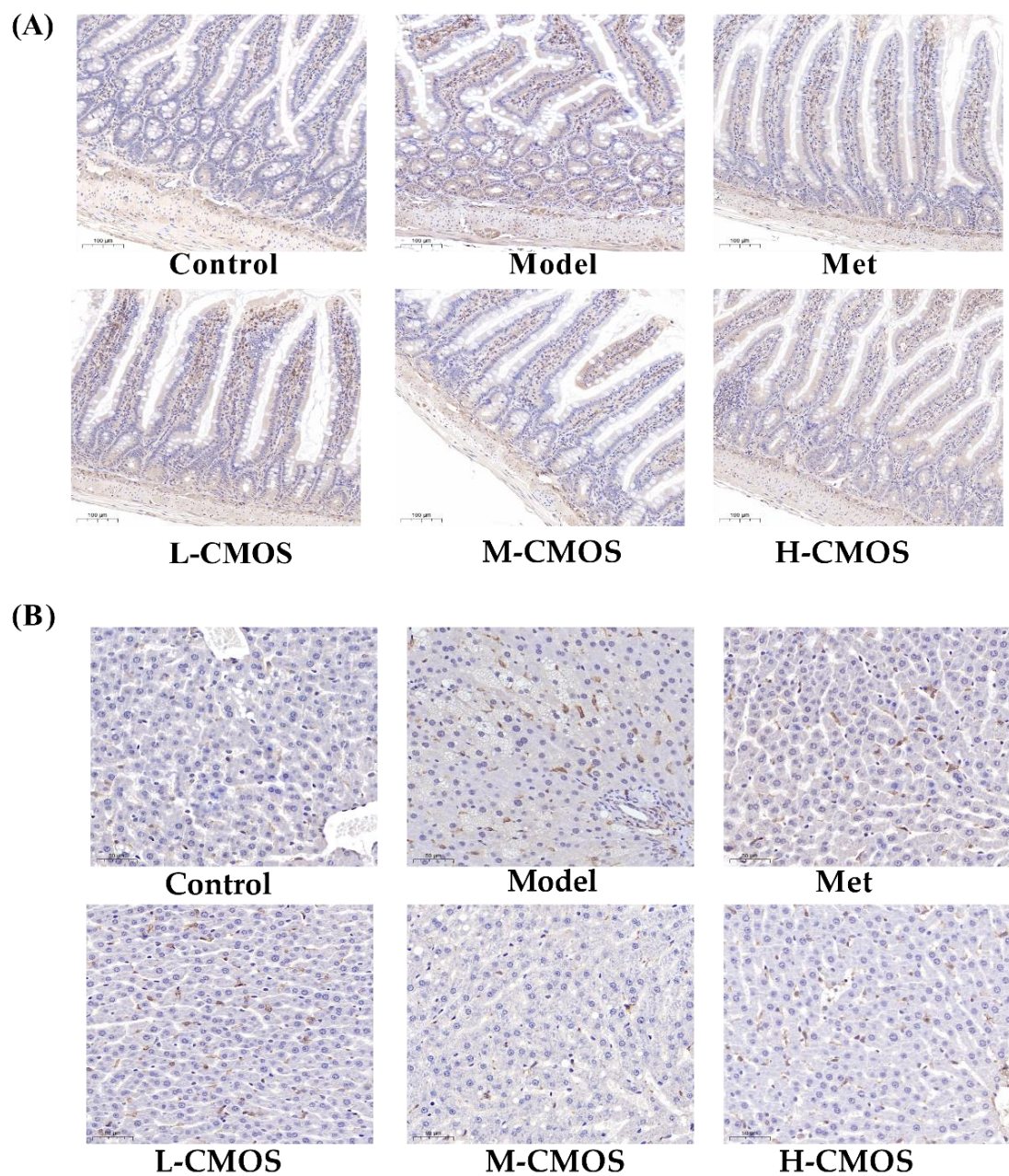


Figure S1. F4/80 immunohistochemical staining (n = 3). For a negative control of the nonspecific fluorescent signal, tissue sections were incubated with 10% normal goat serum instead of primary antibody. Representative photomicrographs of F4/80 immunostaining of (A) ileum (magnification 100×) and (B) liver (magnification 200×).

Spearman Correlation Heatmap

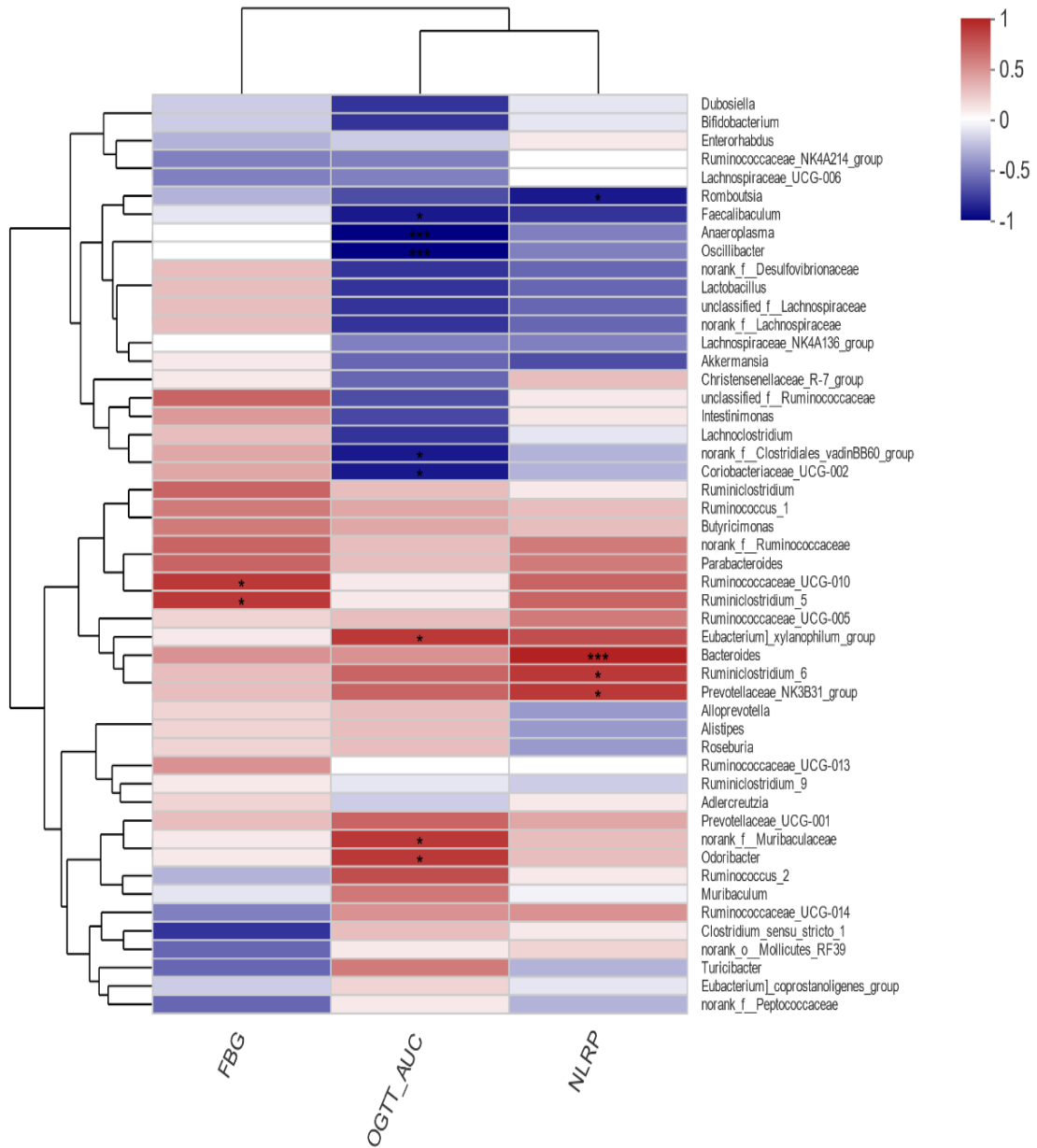


Figure S2. Effects of CMOS treatment on gut microbiota structure in STZ plus HFSD- induced rats (n = 5). Heatmap of the correlation between gut microbiota and environmental factors at the level of CMOS group, showing the color gradient from blue (low abundance) to red (high abundance), and “*” ($p < 0.05$) indicates significance.

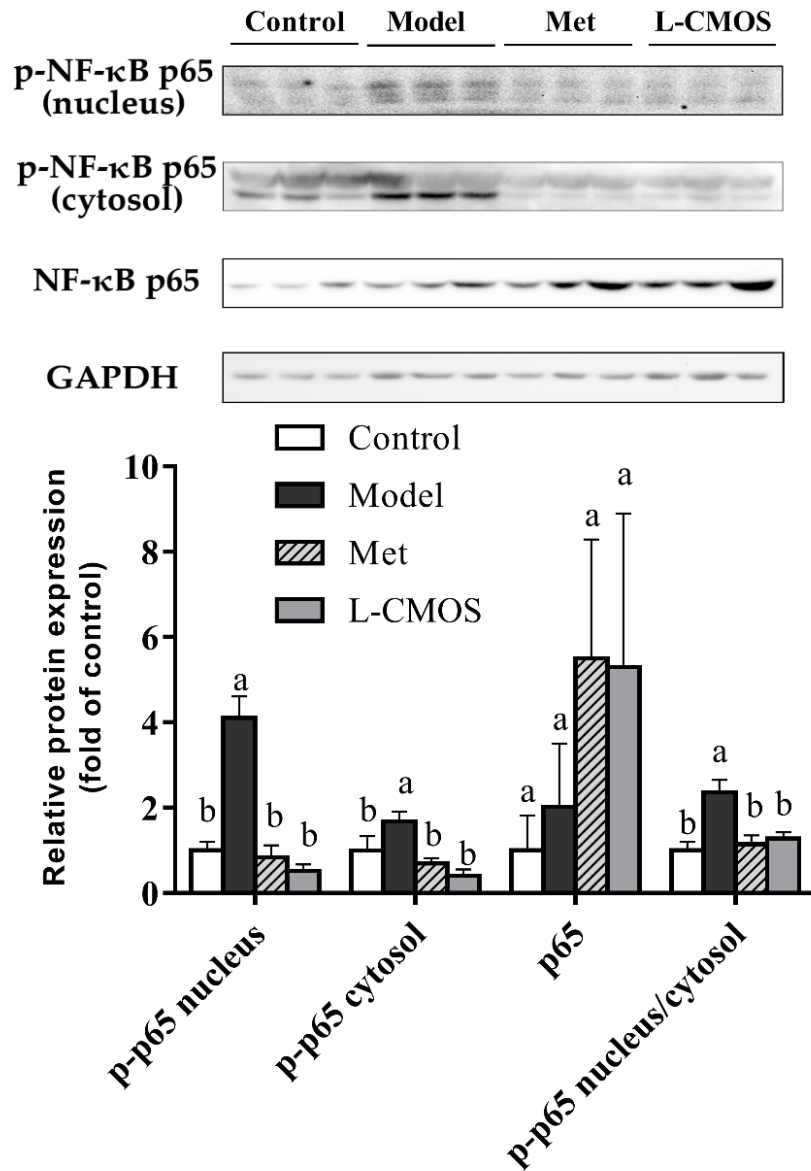


Figure S3. Effects of CMOS on the activation of NF-κB p65 in liver of STZ plus HFSD-induced rats. Western blot images of p-NF-κB p65 and NF-κB p65 in nucleus and cytosol. The level of p-NF-κB p65 and NF-κB p65 was measured by protein band density using ImageJ software. Each value represents the mean \pm SD ($n = 3$). Values with different letters (a-b) are significantly different with each other ($p < 0.05$).

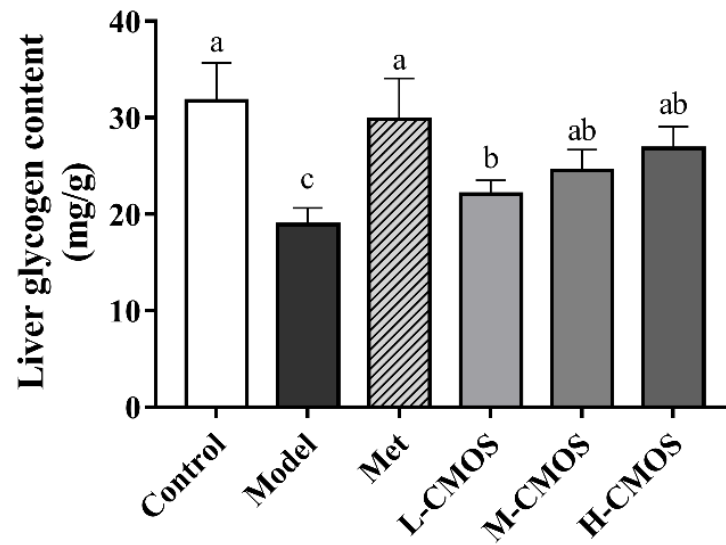


Figure S4. Effects of CMOS on liver glycogen in STZ plus HFSD-induced rats. Each value represents the mean \pm SD ($n = 6$). Values with different letters (a-c) are significantly different with each other ($p < 0.05$).

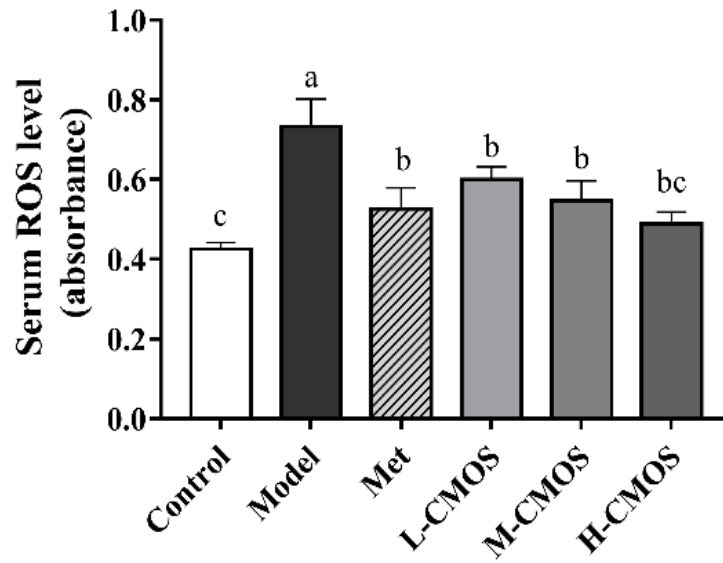


Figure S5. Effects of CMOS on serum ROS production in STZ plus HFSD-induced rats.

Results were represented as mean \pm SD (n = 10) of three independent measurements. Values

with different letters (a-c) are significantly different with each other ($p < 0.05$).

Table S1 Effects of CMOS treatment on food intake, energy intake, and food efficiency ratio in STZ plus HFSD-induced rats*

	Initial body weight (g)	Final body weight (g)	Food intake (g)	Energy intake (kcal/d)	FER (B.W gain/ Food intake)
Control	195.8 ± 12.9 ^a	325.3 ± 14.2 ^b	14.70 ± 0.9 ^a	52.92 ± 3.1 ^c	10.2 ± 0.6 ^b
Model	236.1 ± 21.2 ^a	476.5 ± 34.7 ^a	13.56 ± 0.7 ^a	61.02 ± 2.2 ^a	14.0 ± 1.8 ^a
Met	245.3 ± 17.8 ^a	389.4 ± 19.3 ^b	11.35 ± 0.7 ^c	51.08 ± 2.4 ^c	8.3 ± 0.8 ^c
L-CMOS	259.7 ± 15.1 ^a	439.3 ± 24.5 ^b	12.48 ± 0.9 ^{bc}	56.16 ± 2.1 ^b	11.6 ± 0.7 ^b
M-CMOS	254.4 ± 20.6 ^a	427.5 ± 22.8 ^b	12.62 ± 0.4 ^{bc}	56.79 ± 1.3 ^b	10.6 ± 0.9 ^b
H-CMOS	256.2 ± 20.7 ^a	410.1 ± 26.7 ^b	11.68 ± 0.8 ^c	52.56 ± 2.7 ^c	9.8 ± 1.5 ^{bc}

*The initial body weight, final body weight, and food intake of the rats during the gavage were monitored, and food efficiency ratio (FER) was calculated at the end of the administration. Results were represented as mean ± SD (n = 10). Values with different letters (a-c) are significantly different with each other ($p < 0.05$).